Biosensors and Bioelectronics 86 (2016) 892–898

Contents lists available at ScienceDirect

Biosensors and Bioelectronics

journal homepage: www.elsevier.com/locate/bios

Trifunctional molecular beacon-mediated quadratic amplification for highly sensitive and rapid detection of mercury(II) ion with tunable dynamic range ☆

Yue Zhao, Huaqing Liu, Feng Chen, Min Bai, Junwu Zhao *, Yongxi Zhao *

The Key Laboratory of Biomedical Information Engineering of Ministry of Education, School of Life Science and Technology, Xi'an Jiaotong University, Xi'an, Shaanxi, 710049 PR China

ARTICLE INFO

Article history:
Received 26 May 2016
Received in revised form
18 July 2016
Accepted 27 July 2016
Available online 28 July 2016

Keywords:
Quadratic amplification
Trifunctional molecular beacon
Tunable dynamic range
Mercury(II) ion

ABSTRACT

Analyses of target with low abundance or concentration varying over many orders of magnitude are severe challenges faced by numerous assay methods due to their modest sensitivity and limited dynamic range. Here, we introduce a homogeneous and rapid quadratic polynomial amplification strategy through rational design of a trifunctional molecular beacon, which serves as not only a reporter molecule but also a bridge to couple two stage amplification modules without adding any reaction components or process other than basic linear amplification. As a test bed for our studies, we took mercury(II) ion as an example and obtained a high sensitivity with detection limit down to 200 pM within 30 min. In order to create a tunable dynamic range, *homotropic* allostery is employed to modulate the target specific binding. When the number of metal binding site varies from 1 to 3, signal response is programmed accordingly with useful dynamic range spanning 50, 25 and 10 folds, respectively. Furthermore, the applicability of the proposed method in river water and biological samples are successfully verified with good recovery and reproducibility, indicating considerable potential for its practicality in complex real samples.

1. Introduction

Isothermal nucleic acids amplification efficiently accumulates sequences of interest at constant temperature, and has been successfully applied to the detection of nucleic acids and non-nucleic acid analytes (Li et al., 2010; Zhang et al., 2015, 2014c; Zhao et al., 2015). In contrast to the traditional assay at a target-to-signal ratio with 1:1 stoichiometry (one target converts only one signal readout), isothermal amplification-based biosensors significantly improve the detection sensitivity (Ge et al., 2014b; Liu et al., 2015; Zhang et al., 2014b). According to reaction kinetics, the existing approaches can be mainly classified into two types: exponential and polynomial (linear or quadratic) ones. Exponential strategies exhibit exceedingly high amplification efficiency offering a superior sensitivity (Ma et al., 2014; Tian and Weizmann, 2012). Nevertheless, these methods involve the weaknesses of non-specific amplification primarily caused by interaction between template and DNA polymerase in the absence of target, so that suffer reproducibility problems from the assay of low-abundance analytes. Various linear amplification methods have been proposed and widely applied for their robustness and simplicity, yet are not adequate to detect trace targets due to their inherent low magnification of 1:N (Deng et al., 2014; Ge et al., 2014a). Quadratic strategies cascade two or more amplification modules together, achieving a predominant sensitivity even comparable with those of exponential ones, and have attracted considerable attention (Duan et al., 2013; Ye et al., 2014). On the basis of its enhanced amplification ratio of 1:N^2, several novel approaches have been successively developed (Yu et al., 2014; Wang et al., 2013). Notably, our group has designed a quadratic DNA machine by integrating two linear amplification modules into a one-step biosensing system via a bifunctional hairpin probe. Though it works well in the detection of lead ion and DNA adenine methylation methyltransferase, the thermodynamic equilibrium associated with enthalpy and entropy of stem-loop structure complicates its design (Zhao et al., 2014). Further, we upgraded the quadratic DNA machine utilizing a phosphorothioate-modified amplification template without adding any component other than linear amplification. However, an extra chemical modification still makes the preprocessing tedious (Chen et al., 2015a). Thus, it is urgently needed to develop a simple and homogeneous quadratic

☆The authors declare no competing financial interest.

* Corresponding authors.
E-mail addresses: nanoptzhao@163.com (J. Zhao), yxzhao@mail.xjtu.edu.cn (Y. Zhao).

http://dx.doi.org/10.1016/j.bios.2016.07.099
0956-5663/

amplification strategy.

Apart from sensitivity, a tunable dynamic range (defined here as the ratio between target concentration at which sensor response transits from 10% to 90% of its signal output) is equally important for practical application as analytes concentrations in diverse samples cover several orders of magnitude (Clausson et al., 2011; Law, 1992). Typically, a set of ligands varying in affinity were utilized to edit the dynamic range of biosensors (Vallée-Bélisle et al., 2012; Zhang et al., 2014a). In spite of their impressive performances, the design and generation for series of recognition elements (often of unknown structure) with appropriate target affinity represents a major obstacle for their routine applications. Sequestration mechanism has also been adapted to narrow dynamic range and obtain a steep response such as for reducing noise in molecular logic gates (Kang et al., 2012; Lou et al., 2013). Whereas, signal presents only if target accumulates enough to saturate depletant and surpasses the concentration threshold, which affects the limit of detection. Inspired by the responsive allostery of nature receptors after ligand binding, an alternative dynamic range programmed approach through controlling the *homotropic* effectors has been developed (Porchetta et al., 2013; Simon et al., 2014).

Herein, we construct a trifunctional molecular beacon (TMB) mediated quadratic amplification (TMBQA) strategy with tunable dynamic range. In this homogeneous reaction, a TMB is tactfully designed not only for reporting signal but also bridging the upstream target triggered amplification and the downstream self-templated amplification. For the exploration of our design approach, we take mercury(II) ion (Hg^{2+}), which is a hazardous pollutant with bioaccumulation and strong toxicity, as a model analyte. Once thymine (T)-Hg^{2+}-T coordination forms, the upstream amplification is triggered and continuously yields a great amount of DNA products complementary with the priming domain at 3′ terminal region of TMB, inducing a significant enhancement of fluorescence response as well as initiating the downstream amplification templated by TMB. Similar with upstream, the products of downstream anneals with cascade amplification domain at 5′ terminal region of TMB and lead more fluorescence restoration within short assay time (30 min), thus exhibit an excellent sensitivity with limit detection of 200 pM in one step. In addition, the dynamic range of sensor has been successfully tuned through controlling the number of Hg^{2+} specific binding sites via *homotropic* allostery. Since one target facilitates the binding of subsequent ones, the signal response of multivalent receptor displays a positive cooperativity so that the useful dynamic range has been arbitrarily engineered to extend or narrow. Finally, we tested the proposed sensor with complex real samples and obtained results accordance with Atomic Fluorescence Spectrometry (AFS), demonstrating its accuracy and reliability in practical application.

2. Experimental section

2.1. Reagents and Materials

Mercury perchlorate trihydrate ($Hg(ClO_4)_2 \cdot 3H_2O$) was obtained from J&K Chemical Ltd. (Beijing, China). NaAc, KAc, $Mg(Ac)_2$, $BaCl_2$, $NiSO_4$, $FeCl_2$, $ZnCl_2$, $MnSO_4$, $CaCl_2$, $Pb(NO_3)_2$, $FeCl_3$, $AlCl_3$, 3-(*N*-morpholino)-propanesulfonic acid (MOPS), Tris(hydroxymethyl)aminomethane (Tris) and other chemicals were purchased from Sinopharm Chemical Reagent Co., Ltd. (Shanghai, China). Klenow Fragment (exo^-), Nt. BbvCI and their corresponding buffer were ordered from New England Biolabs Ltd. (Beijing, China). All the oligonucleotides were synthesized by Sangon Biotechnology Co., Ltd. (Shanghai, China). The sequences are listed in Table S1 (Supporting Information). All solutions were prepared and diluted with Milli-Q water (resistance $> 18.2\ M\Omega$).

2.2. Apparatus

Fluorescence measurements were carried out on FluoroMax-4 fluorescence spectrometer (Horiba Jobin Yvon, Edison, NJ). Excitation and emission wavelengths were set at 494 nm and 518 nm with the slit widths of 5 nm, respectively. The emission spectra were monitored from 510 nm to 600 nm in steps of 1 nm. LightCycler 96 (Roche Applied Science, Mannheim, Germany) was used to record melting curves.

2.3. Analysis of samples

Hg^{2+} stock solution (10 mM) was prepared by dissolving $Hg(ClO_4)_2 \cdot 3H_2O$ with 0.5% HNO_3, further diluted to desired concentration with 10 mM MOPS solution (pH = 7.0) containing 0.1 M $NaNO_3$. The detection was carried out in a Tris-Ac buffer (10 mM Tris, 50 mM KAc, 10 mM $Mg(Ac)_2$, pH = 7.9) containing 40 nM primer, 40 nM template, 150 nM TMB, 0.75 units Klenow Fragment, 4 units Nt.BbvCI and 40 μM dNTPs. After addition of various concentrations of Hg^{2+}, the solutions were incubated at 37 °C for 30 min. Then fluorescence emission spectra were recorded as described above.

MCF-7 cells were incubated with high glucose medium (H-DMEM) supplemented with 10% Fetal Bovine Serum (FBS) in an atmosphere of 5% CO_2 at 37 °C. Cells were cultured to 70–80% confluence and collected after trypsin digestion. Then the collected cells were washed twice and suspended in phosphate-buffered saline (PBS, pH = 7.4). Cell lysis (approximately 7.5×10^5 cells) was performed by sonication to make cells homogeneous, and then centrifuged to collect supernatant. Human serum samples were obtained from Xi'an Jiaotong University Hospital.

3. Results and discussion

3.1. Design of TMBQA strategy

As illustrated in Scheme 1, a TMB is tactfully designed as a bridge to cascade two stage amplification modules. Then the upstream Hg^{2+} triggered amplification and the downstream self-templated amplification are integrated into a one-step homogeneous system without adding any reaction components or process other than basic linear amplification. The primer-template complex probe contains variable number of T-T mismatches (denoted as red and cyan) by which Hg^{2+} specific binding is modulated. Once induced by T-Hg^{2+}-T coordination (circled by dash line), primer offers a complementary 3′ terminal to initiate polymerization. Upon the subsequent operation of repeated scission and replication, numerous of upstream DNA products are generated. These products can anneal with priming domain I (highlighted in green) at 3′ terminal region of TMB and lead a significant fluorescence restoration. Then the upstream products primed-downstream amplification is started synchronously taking TMB as a template, producing duplex sequence containing the recognition domain II (highlighted in orange) for Nt.BbvCI. The cleavage results in a new extension to continue displacement and release downstream DNA products which can hybridize with another TMB at cascade amplification domain III (highlighted in violet) of its 5′ terminal region, yielding a quadratic amplified detection signal. Therefore, a simple and homogeneous quadratic amplification strategy with tunable dynamic range is presented.

In theory, we refine the amplification mathematical model of our proposed method and describe the signal equations as $Y_1 = N$

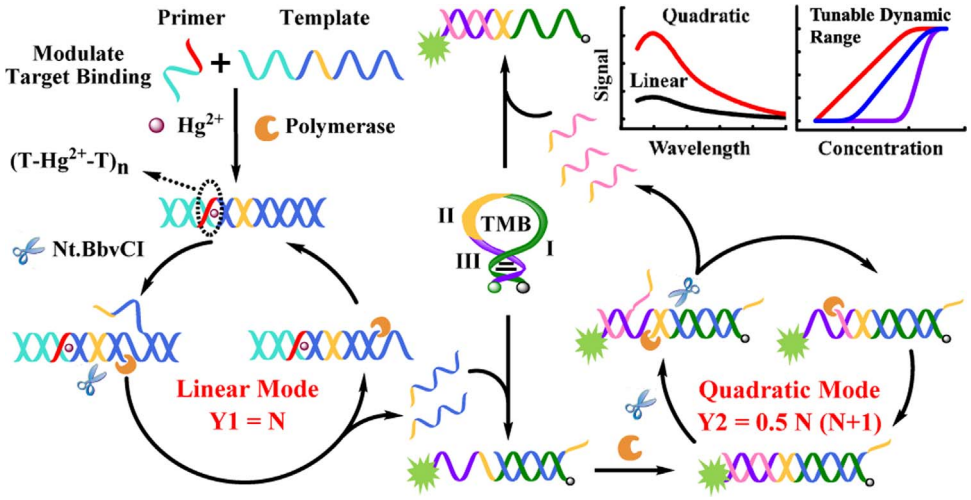

Scheme 1. Schematic illustration of TMBQA and its application for Hg^{2+} detection with tunable dynamic range. I, II, III in the TMB represent priming domain, recognition domain and cascade amplification domain, respectively. (For interpretation of the references to color in this figure, the reader is referred to the web version of this article)

for the upstream linear mode and $Y_2 = 0.5\ N\ (N+1)$ for the cascade quadratic mode, where Y_1 and Y_2 represent the signal intensity of each mode respectively, and N is the cycle number. Note that Y_2 is always greater than Y_1 when $N > 1$ (Table S2 and Fig. S1).

To evaluate the amplification efficiency of different modes, we compared their fluorescence response using standard complementary primer (C-primer). In the linear process, we prolonged the quadratic template with extra 3 bases at its 5′ terminal to ensure the upstream amplification products unable to primed downstream amplification. As expected, the quadratic mode exhibits an excellent signal enhancement superior to that of the linear (Fig. S2). For the detection of Hg^{2+}, Primer8, which contains single Hg^{2+} binding site is involved. In the presence of Hg^{2+}, Primer8 and template form duplex structure with Hg^{2+}-mediated base pair to initiate amplification. As presented in Fig. 1(A), the addition of Hg^{2+} (20nM) in the TMBQA system induced a 12.7-fold fluorescence signal enhancement, whereas only a 3.3-fold signal increase was achieved by the linear mode. In addition, the TMBQA products were investigated by agarose gel electrophoresis and melting curve. An obvious products band is observed in lane b other than lane a, which are mixture of the assay system with and without Hg^{2+}, respectively. Corresponding melting curve analysis also depicts the consistent results (Fig. 1B).

3.2. Optimization of assay conditions

To achieve the best sensing performance, ionic strength of buffer solution and tool enzyme concentrations were investigated at a fixed Hg^{2+} concentration of 20 nM. As a result, 50 mM KAc, 10 mM Mg $(Ac)_2$, 0.75 units Klenow Fragment, 4 units Nt. BbvCI were selected to obtain the maximum fluorescence enhancement (F/F_0) (data were shown in Supporting information Fig. S3). Moreover, several key parameters were further optimized through a series of experiments.

The concentration of primer-template complex probe was tested as depicted in Fig. S4(A), from which we can see similar F/F_0 from 10 nM to 40 nM. It's possible that increased reactant concentration accelerates reaction rate but in turn provides more available templates to compete with TMB for occupying amplification products. Thereby, 40 nM probe is selected and utilized in

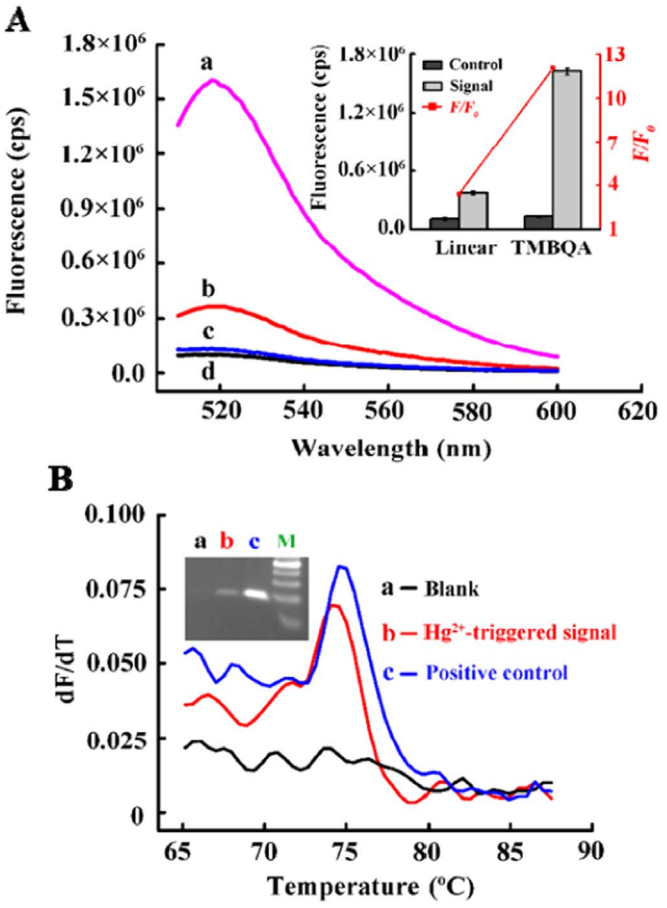

Fig. 1. (A) The fluorescence spectra of the TMBQA (a) and basic linear amplification system (b) in the presence of 20nM Hg^{2+}, with corresponding backgrounds control without Hg^{2+} (c, d), respectively. Inset: The fluorescence responses of quadratic amplification and basic linear amplification. The error bar indicates the SD from three independent experiments and the SD is less than 0.35 ($\times 10^5$cps). (B) Gel electrophoresis and melting curve analysis: lane a, TMBQA without Hg^{2+}; lane b, TMBQA with Hg^{2+}; lane c, positive control with complementary primer; M, the 20bp DNA ladder marker range from 20 to 100bp.

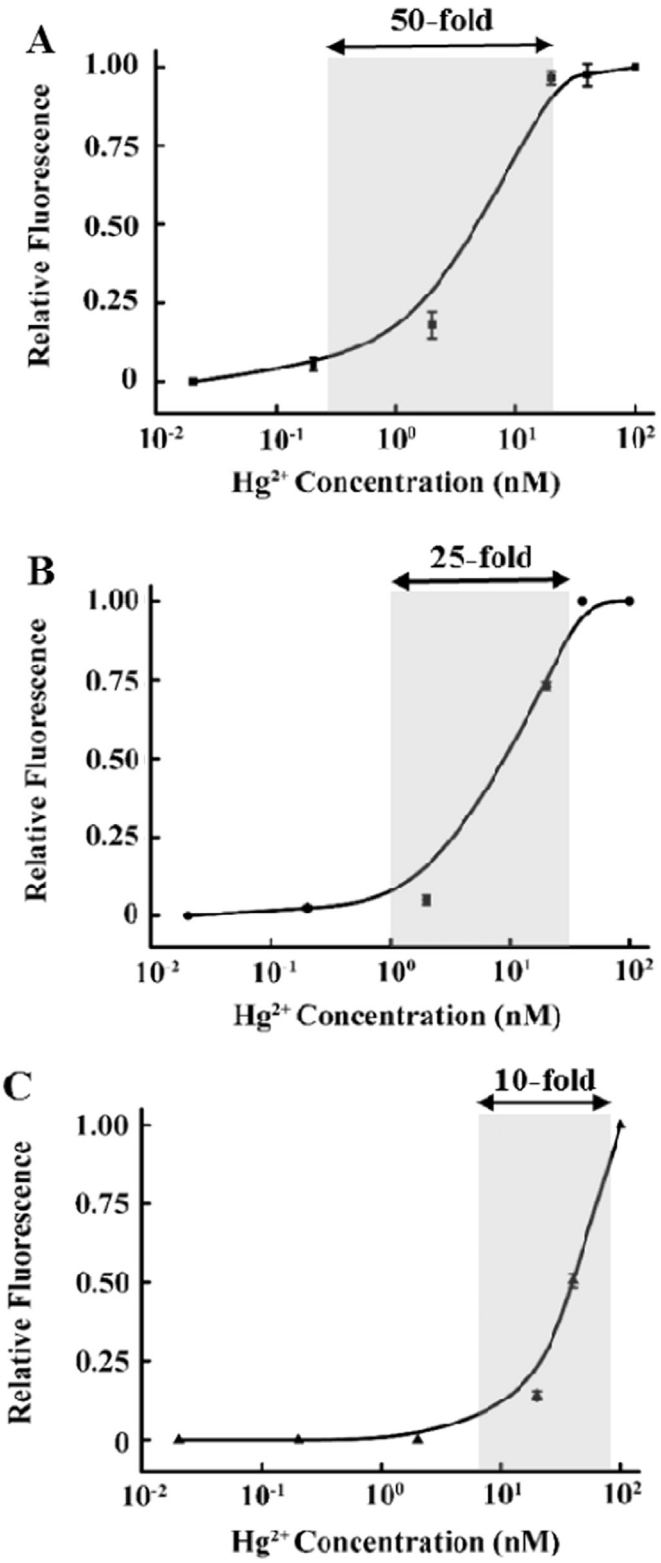

Fig. 2. Modulation of the dynamic range by controlling target binding via *homotropic* allostery. Monovalent probe (with single site) presents a dynamic range spaning 50 folds (A), bivalent probe (with double sites) narrows the dynamic range to 20 folds (B), and trivalent probe (with ternary sites) produces a very steep response curve with dynamic range of 10 folds (C). The error bar indicates the SD from three independent experiments and the SD is less than 0.04.

the following experiments. Additionally, amplification capability was investigated at different reaction time. It is clearly seen in Figure. S4(B), the fluorescence response is quickly enhanced within 30 min and remains almost unchanged with time prolongs. On the basis of the highest value of F/F_0, 30 min is employed.

3.3. Modulation of dynamic range

Biomolecular recognition is often achieved via allosteric cooperativity, a process in which sequential recognition events on a multivalent receptor are coupled so that the initial one enhances the binding of the subsequent, leading a steep response than those observed at monovalent receptors (Porchetta et al., 2013; Simon et al., 2014). Thus, to obtain an appropriate dynamic range covering Hg^{2+} concentrations in different environments, we modulated the number of binding sites in primer-template complex probe from 1 to 3. By employing a monovalent probe with single binding site (Primer9), a highly sensitive sensor, for which the useful dynamic range spanning from 0.4nM to 20nM is created (Fig. 2A). Due to the positive cooperation of *homotropic* allostery, the second binding site (M2-primer9) leads a steeper response with dynamic range falls to 20-fold as shown in Fig. 2(B). Encouraged by this successful design efforts, we next adapted trivalent probe (M3-primer9) containing ternary binding sites to edit the dynamic range. As expected, this process is quite synergetic, exhibiting an approximately "all-or-nothing" digital-like response curve (Fig. 2C).

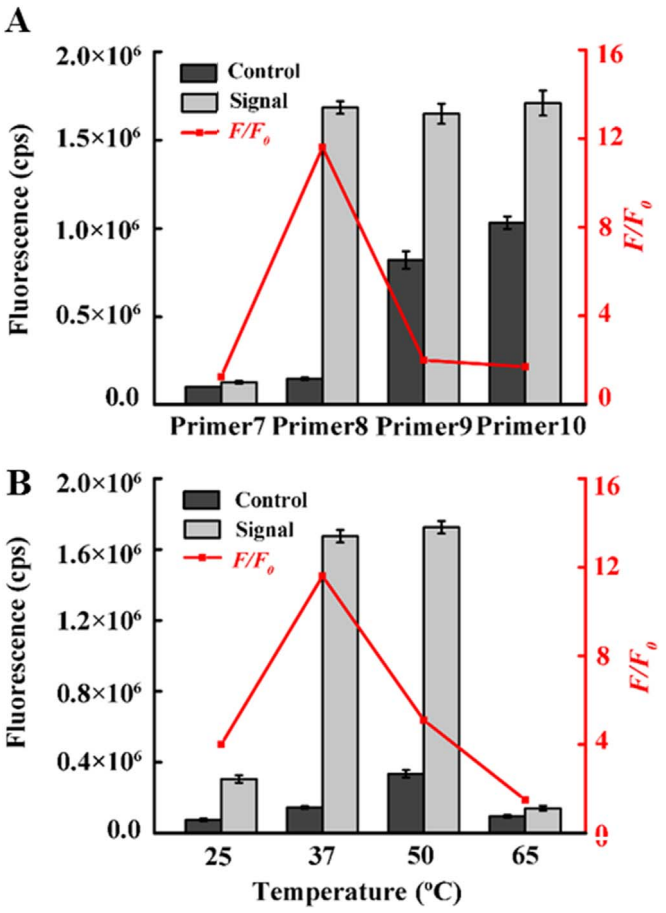

Fig. 3. To explore the relationship between thermodynamics properties and the amplified performance, we have fabricated a set of primer-template probes (A) and investigated the binding affinity of polymerase and stability of primer-template duplex at different temperature (B). The error bar indicates the SD from three independent experiments and the SD is less than 0.71 ($\times 10^5$cps).

3.4. Thermodynamics regulation

Primer and template are at an equilibrium between dissociative state and duplex state (a binding-competent conformation for Hg^{2+}). Through investigating thermodynamic stability of primer-template complex, the Hg^{2+} triggered TMBQA can be regulated. As shown in Fig. 3(A), 7-mer primer (Primer7) exhibits no significant fluorescence signal as well as blank control. Then the signal abruptly increases with the primer length added to 8-mer (Primer8). When the length of primer reaches up to 9 (Primer9) and 10 (Primer10), signal shows no further enhancement whereas unwanted background fluorescence presents a remarkable growth. Undoubtedly, 8-mer primer was employed for the following experiments due to the highest F/F_0. Further, we try to explain the phenomena appear at 7-mer and 9-mer primer. Firstly, we consider the thermodynamics stability of primer-template duplex, and attribute both the negligible signal and background to the failure of hybridization. According to the empirical formulae for evaluating melting temperature (T_m) of primer less than 25-mer ($T_m = 4 \times (G+C) + 2 \times (A+T)$; G, C, A, and T indicate the number of corresponding nucleotides in the primer.), one added base elevates T_m about 2–4°C thus indeed ensure a better stability. To verify our assumption, we compared the performance of Primer8 at four temperatures, namely 25°C, 37°C, 50°C and 65°C (Fig. 3B). To our surprise, we found TMBQA even exhibits a preferable amplification efficiency at 50°C (much higher than its T_m). If T_m is the determinant to lead significant difference between Primer7 and Primer8 (only a difference of 2°C), the performance at 50°C seems beyond of understanding. On account of polymerization is not only based on an absolutely stable hybridization but also can be triggered by transient duplex formation (Tsai et al., 2007), we paid close attention to the recognition behavior of polymerase. In general, polymerases share a global architecture and short primer-template duplex reduces its binding affinity (Zhao and Guan, 2010). So we surmise only if the complementary region reaches up to 8bp, the primer can be recognized by polymerase and initiates amplification in our proposed system. 7-mer primer is unable to extend as its length is shorter than the minimal requirement. 8-mer primer exhibits significant fluorescent response with negligible background for the duplex length of primer-template complex is just across the critical point before and after binding Hg^{2+}. In addition, we have previously investigated the impact of various 3′-terminal mismatches on amplification and demonstrated T-T mismatch presents an ability to induce nonspecific extension (Chen et al., 2015b). So, if provided allowable complementary length such as Primer9 and Primer10, an undesirable background fluorescence is generated seriously. Eventually, through investigating the stability of primer-template duplex and binding affinity of polymerase, we regulated the thermodynamics of TMBQA, and provided an optimum structure for the subsequent experiments.

3.5. Detection of Hg^{2+} based on TMBQA

Some representative nucleic acid amplification strategies have already been applied for the detection of Hg^{2+}. Zhou et al. described a highly sensitive electrochemiluminescent sensor based on Hg^{2+}-mediated rolling circular amplification (Zhou et al., 2012). Yin et al. presented a label-free method for the detection of Hg^{2+} using DNA molecular machine-based fluorescent silver nanoclusters (Yin et al., 2013). Among these, it is worthwhile to point out an important factor, dithiothreitol (DTT), which is commonly used in the stock solutions and reaction buffers of almost all commercial tool enzymes including Klenow Fragment and Nt. BbvCI used in our reactions. However, it is widely reported that DTT is a strong chelating reagent and the thiol groups of which easily form specific and very stable complexes with Hg^{2+}, thus can be used to sequestrate Hg^{2+} (Chaudhary et al., 2015; Thomas et al., 2012). Similar problems have also been mentioned in some related research. Li et al. (Li et al., 2008) and Zhu et al. (Zhu et al., 2011) utilized DTT with one-thousandth concentration of the supplied buffer to alleviate the interference. Liu et al. (Liu et al. 2014) even took out this component from their reaction systems, and confirmed it was unnecessary for enzyme's normal function. However, all these strategies above can't rule out the DTT introduced by enzyme from their stock buffers, which is normally 1–10mM (far above the Hg^{2+} concentration in routine samples). As the strong reducing property of thiol, we try to eliminate it by oxidant and give priority to H_2O_2 for its reduction product is H_2O, which would not introduce interference to reaction (Winterbourn and Metodiewa, 1999). As shown in Fig. 4(A), the concentration of H_2O_2 added was optimized from 0.1% to 10%. When the concentration is below 0.3%, fluorescence intensity drops for the Hg^{2+} is grabbed by DTT. With the increase of H_2O_2, a significant fluorescence enhancement is acquired, indicating DTT has been gradually oxidized and Hg^{2+} is available to trigger the amplification. Ascribe to the destructive effect of strong oxidant, excessive H_2O_2 weakens the fluorescence intensity, so we set 3% H_2O_2 (with no adverse effect on standard amplification system, Fig. S5) as the optimum condition.

Under the optimized assay conditions, a high sensitivity was demonstrated by testing a series of samples containing different Hg^{2+} concentrations. As can be seen in Fig. 4(B), the fluorescence intensity increases with the concentration of Hg^{2+} varied from 0 to 40 nM. In terms of the rule of 3 times standard deviation over the blank response, the detection limit is down to 200 pM, which is much lower than the maximum level (10 nM) of Hg^{2+} in drinking water permitted by the Environmental Protection Agency. The Fig. 4(C) clearly illustrates a good linear relationship between the fluorescence intensity of 518 nm and the concentrations of Hg^{2+} up to 20 nM. With a correlation coefficient of 0.9938, the corresponding regression equation is $Y = 0.7233X + 1.55$, where Y is the fluorescence intensity ($\times 10^5$ cps) and X is the Hg^{2+} concentration. To further demonstrate precision of this proposed assay, we calculated the inter- and intra-assay imprecisions of this assay from 3 independent experiments at Hg^{2+} concentration of 10 nM. The CV values are 3.4% and 2.5%, respectively.

Traditional methods such as AFS (Leopold et al., 2009) and inductively coupled plasma mass spectrometry (ICP-MS) (Rodrigues et al., 2010) offer high sensitivity and selectivity for Hg^{2+} quantification, and have been extensively applied in complex real samples. However, due to the pronounced absorbency of Hg^{2+}, these above methods suffer from a memory effect, wherein Hg^{2+} accumulates within the flow injection apparatus and is slowly released over time to adversely affect the detection (Li et al., 2006; Zhang et al., 2011). As an alternative approach, TMBQA is highly promising for its accuracy, specificity and low-cost. Since the closed-tube reaction were kept at microliter volumes in the disposable containers, contamination attributed to Hg^{2+} adsorption on the transfer tubing, spray chamber and nebulizer can be avoided. In addition, compared with those methods requiring sophisticated instruments, fluorescent sensors are easy to miniaturize and hold great potential for implementing on field detection by combining with the portable fluorescence spectrophotometers.

To evaluate the selectivity of this proposed method, fluorescence response of Hg^{2+} to that of other environmentally relevant metal ions such as K^+, Na^+, Mg^{2+}, Ba^{2+}, Ni^{2+}, Fe^{2+}, Zn^{2+}, Mn^{2+}, Ca^{2+}, Pb^{2+}, Al^{3+} and Fe^{3+} were compared. As revealed in Fig. 4 (D), an obvious fluorescence response is observed from the solution in the presence of 20 nM Hg^{2+}, while other metal ions (2 μM) exhibit almost the same fluorescence intensity as blank control. Thus, these results prove that the sensing strategy has a good

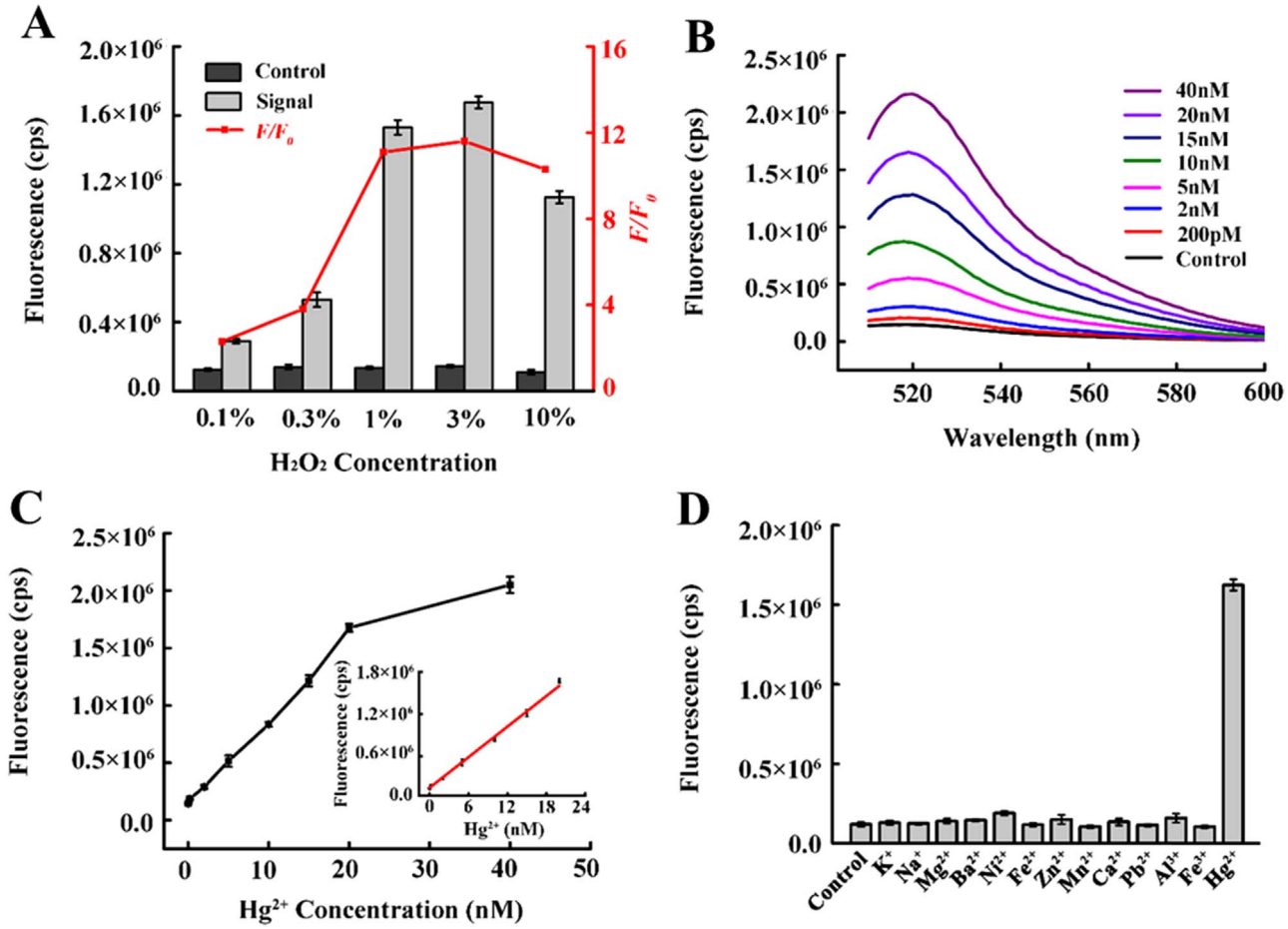

Fig. 4. (A) Effect of H_2O_2 concentration on the TMBQA-based Hg^{2+} detection. (B) Fluorescence emission spectra in the presence of different concentrations of Hg^{2+} ranging from 0 to 40nM. (C) The relationship of the fluorescence intensity with various Hg^{2+} concentrations. The inset displays the linear correlation between fluorescence intensity and Hg^{2+} concentrations up to 20nM. (D) Selectivity of the sensing strategy for Hg^{2+} detection over other common interference metal ions. The concentration of Hg^{2+} is 20nM, whereas the concentrations of other metal ions are each 2μM. The error bar indicates the SD from three independent experiments and the SD is less than 0.71 ($\times 10^5$cps).

Table 1
Results for the Hg^{2+} determination in river water samples.

Sample	Added (nM)	AFS (nM)	Recovery (%)	Proposed method (nM)	Recovery (%)
1	5	5.32 ± 0.46	106.4	4.55 ± 0.21	91.0
2	10	10.05 ± 0.42	100.5	9.75 ± 0.35	97.5
3	15	14.78 ± 0.17	98.5	15.2 ± 0.63	101.3

Mean values and SDs were obtained from three independent experiments.

specificity to Hg^{2+} over other competing metal ions.

To determine the potential practicability of the proposed strategy, we simply filtered the Xi'an Chan River collected water samples by a 0.22 μm membrane and observed no signal response of Hg^{2+}, which has been confirmed by AFS. To further investigate the assay's practical application in real water sample, we applied it to artificially contaminated water samples spiked with different concentrations (5, 10, 15 nM) of Hg^{2+}. As listed in Table 1, the recovery and standard deviation of these water samples were satisfactory, demonstrating this method is reliable and practical.

As another classic and common application area of biosensors, biological sample analysis have attracted more and more attentions. Nucleic acid amplification-based Hg^{2+} biosensors not only have shown good performance in real water samples, but also hold great potential in biological samples due to their minimized sample consumption and mild reaction conditions. To evaluate the feasibility of proposed method in biological samples, the detection of Hg^{2+} in cell extract and human serum samples were performed. The treated cell extract and 1:50 diluted serum samples were firstly tested by AFS to obtain the initial concentration of Hg^{2+}, and then spiked with Hg^{2+} at three different concentrations (5, 10, 15 nM). In order to eliminate the interferences of biothiols in biological samples and improve recoveries, samples were mixed with H_2O_2 (about 3%) before detection. As summarized in Table S3, the recoveries of Hg^{2+} are in the range 95.8–101.9%, validating the potential value of the proposed method for detecting Hg^{2+} in complex biological samples.

4. Conclusions

In summary, we have developed a simple and one-step TMBQA strategy with tunable dynamic range and applied it on the detection of Hg^{2+}. In this homogeneous reaction, TMB is specially designed as a bridge between the upstream target triggered amplification and the downstream self-templated amplification besides its original function as signal reporter. *Homotropic* allostery are employed to modulate the dynamic range and an accurate quantification of Hg^{2+} over different concentrations was achieved. Without any troublesome procedures, the strategy exhibits a high sensitivity of picomolar level and tunable detection range within 30 min. Furthermore, the sensing strategy was successfully used to

detect real water and biological samples with satisfactory recovery, holding great potential for its application in complex real samples. Upon proper modification of the recognition element, this proposed method can be extended to the sensitive and convenient detection of other analytes at different concentration levels, thereby promising a new avenue for the assay of various types of targets.

Acknowledgments

This research was financially supported by the Research Project Foundation of Shaanxi Branch of China National Tobacco Corporation (No. 201112029), the National Natural Science Foundation of China (No. 21475102) and "Young Talent Support Plan" of Xi'an Jiaotong University. We would like to thank Engineer Guanghui Qiang at Xi'an Water Group Company Limited (Xi'an, Shaanxi) for supporting the AFS analysis.

Appendix A. Supplementary material

Supplementary data associated with this article can be found in the online version at http://dx.doi.org/10.1016/j.bios.2016.07.099.

References

Chaudhary, A., Dwivedi, C., Chawla, M., Gupta, A., Nandi, C.K., 2015. Lysine and dithiothreitol promoted ultrasensitive optical and colorimetric detection of mercury using anisotropic gold nanoparticles. J. Mater. Chem. C 3 (27), 6962–6965.

Chen, F., Fan, C., Zhao, Y., 2015a. Inhibitory impact of 3′-terminal 2′-O-methylated small silencing RNA on target-primed polymerization and unbiased amplified quantification of the RNA in *Arabidopsis thaliana*. Anal. Chem. 87 (17), 8758–8764.

Chen, F., Zhao, Y., Fan, C., Zhao, Y., 2015b. Mismatch extension of DNA polymerases and high-accuracy single nucleotide polymorphism diagnostics by gold nanoparticle-improved isothermal amplification. Anal. Chem. 87 (17), 8718–8723.

Clausson, C.-M., Allalou, A., Weibrecht, I., Mahmoudi, S., Farnebo, M., Landegren, U., Wählby, C., Söderberg, O., 2011. Increasing the dynamic range of in situ PLA. Nat. Methods 8 (11), 892–893.

Deng, R., Tang, L., Tian, Q., Wang, Y., Lin, L., Li, J., 2014. Toehold-initiated rolling circle amplification for visualizing individual microRNAs in situ in single cells. Angew. Chem. Int. Ed. 53 (9), 2389–2393.

Duan, R., Zuo, X., Wang, S., Quan, X., Chen, D., Chen, Z., Jiang, L., Fan, C., Xia, F., 2013. Lab in a tube: ultrasensitive detection of microRNAs at the single-cell level and in breast cancer patients using quadratic isothermal amplification. J. Am. Chem. Soc. 135 (12), 4604–4607.

Ge, J., Zhang, L.-L., Liu, S.-J., Yu, R.-Q., Chu, X., 2014a. A highly sensitive target-primed rolling circle amplification (TPRCA) method for fluorescent in situ hybridization detection of microRNA in tumor cells. Anal. Chem. 86 (3), 1808–1815.

Ge, Z., Lin, M., Wang, P., Pei, H., Yan, J., Shi, J., Huang, Q., He, D., Fan, C., Zuo, X., 2014b. Hybridization chain reaction amplification of microRNA detection with a tetrahedral DNA nanostructure-based electrochemical biosensor. Anal. Chem. 86 (4), 2124–2130.

Kang, D., Vallée-Bélisle, A., Porchetta, A., Plaxco, K.W., Ricci, F., 2012. Re-engineering electrochemical biosensors to narrow or extend their useful dynamic range. Angew. Chem. Int. Ed. 51 (27), 6717–6721.

Law, P., 1992. Law 102-550. Residential Lead-Based Paint Hazard Reduction Act of.

Leopold, K., Foulkes, M., Worsfold, P.J., 2009. Gold-coated silica as a pre-concentration phase for the determination of total dissolved mercury in natural waters using atomic fluorescence spectrometry. Anal. Chem. 81 (9), 3421–3428.

Li, Y., Chen, C., Li, B., Sun, J., Wang, J., Gao, Y., Zhao, Y., Chai, Z., 2006. Elimination efficiency of different reagents for the memory effect of mercury using ICP-MS. J. Anal. At. Spectrom. 21 (1), 94–96.

Li, D., Wieckowska, A., Willner, I., 2008. Optical analysis of Hg^{2+} ions by oligonucleotide–gold-nanoparticle hybrids and DNA-based machines. Angew. Chem. 120 (21), 3991–3995.

Li, W., Liu, Z., Lin, H., Nie, Z., Chen, J., Xu, X., Yao, S., 2010. Label-free colorimetric assay for methyltransferase activity based on a novel methylation-responsive DNAzyme strategy. Anal. Chem. 82 (5), 1935–1941.

Liu, J., Chen, L., Chen, J., Ge, C., Fang, Z., Wang, L., Xing, X., Zeng, L., 2014. An autonomous T-rich DNA machine based lateral flow biosensor for amplified visual detection of mercury ions. Anal. Methods 6 (7), 2024–2027.

Liu, M., Zhang, W., Zhang, Q., Brennan, J.D., Li, Y., 2015. Biosensing by Tandem Reactions of Structure Switching, Nucleolytic Digestion, and DNA Amplification of a DNA Assembly. Angew. Chem. Int. Ed. 54 (33), 9637–9641.

Lou, X., Zhao, T., Liu, R., Ma, J., Xiao, Y., 2013. Self-assembled DNA monolayer buffered dynamic ranges of mercuric electrochemical sensor. Anal. Chem. 85 (15), 7574–7580.

Ma, F., Yang, Y., Zhang, C.-y, 2014. Ultrasensitive detection of transcription factors using transcription-mediated isothermally exponential amplification-induced chemiluminescence. Anal. Chem. 86 (12), 6006–6011.

Porchetta, A., Vallée-Bélisle, A., Plaxco, K.W., Ricci, F., 2013. Allosterically tunable, DNA-based switches triggered by heavy metals. J. Am. Chem. Soc. 135 (36), 13238–13241.

Rodrigues, J.L., de Souza, S.S., de Oliveira Souza, V.C., Barbosa, F., 2010. Methylmercury and inorganic mercury determination in blood by using liquid chromatography with inductively coupled plasma mass spectrometry and a fast sample preparation procedure. Talanta 80 (3), 1158–1163.

Simon, A.J., Vallée-Bélisle, A., Ricci, F., Plaxco, K.W., 2014. Intrinsic disorder as a generalizable strategy for the rational design of highly responsive, allosterically cooperative receptors. Proc. Natl. Acad. Sci. 111 (42), 15048–15053.

Thomas, J.M., Yu, H.-Z., Sen, D., 2012. A mechano-electronic DNA switch. J. Am. Chem. Soc. 134 (33), 13738–13748.

Tian, L., Weizmann, Y., 2012. Real-time detection of telomerase activity using the exponential isothermal amplification of telomere repeat assay. J. Am. Chem. Soc. 135 (5), 1661–1664.

Tsai, C.-H., Chen, J., Szostak, J.W., 2007. Enzymatic synthesis of DNA on glycerol nucleic acid templates without stable duplex formation between product and template. Proc. Natl. Acad. Sci. 104 (37), 14598–14603.

Vallée-Bélisle, A., Ricci, F., Plaxco, K.W., 2012. Engineering biosensors with extended, narrowed, or arbitrarily edited dynamic range. J. Am. Chem. Soc. 134 (6), 2876–2879.

Wang, F., Freage, L., Orbach, R., Willner, I., 2013. Autonomous replication of nucleic acids by polymerization/nicking enzyme/DNAzyme cascades for the amplified detection of DNA and the aptamer–cocaine complex. Anal. Chem. 85 (17), 8196–8203.

Winterbourn, C.C., Metodiewa, D., 1999. Reactivity of biologically important thiol compounds with superoxide and hydrogen peroxide. Free Radic. Biol. Med. 27 (3), 322–328.

Ye, S., Wu, Y., Zhang, W., Li, N., Tang, B., 2014. A sensitive SERS assay for detecting proteins and nucleic acids using a triple-helix molecular switch for cascade signal amplification. Chem. Commun. 50 (66), 9409–9412.

Yin, J., He, X., Jia, X., Wang, K., Xu, F., 2013. Highly sensitive label-free fluorescent detection of Hg^{2+} ions by DNA molecular machine-based Ag nanoclusters. Analyst 138 (8), 2350–2356.

Yu, C.-Y., Yin, B.-C., Wang, S., Xu, Z., Ye, B.-C., 2014. Improved ligation-mediated PCR method coupled with T7 RNA polymerase for sensitive DNA detection. Anal. Chem. 86 (15), 7214–7218.

Zhang, W.-b, Yang, X.-a, Ma, Y.-y, Zhu, H.-x, Wang, S.-b, 2011. Continuous flow electrolytic cold vapor generation atomic fluorescence spectrometric determination of Hg in water samples. Microchem. J. 97 (2), 201–206.

Zhang, H., Jia, S., Lv, M., Shi, J., Zuo, X., Su, S., Wang, L., Huang, W., Fan, C., Huang, Q., 2014a. Size-dependent programming of the dynamic range of graphene oxide–DNA interaction-based ion sensors. Anal. Chem. 86 (8), 4047–4051.

Zhang, Q., Chen, F., Xu, F., Zhao, Y., Fan, C., 2014b. Target-triggered three-way junction structure and polymerase/nicking enzyme synergetic isothermal quadratic DNA machine for highly specific, one-step, and rapid microRNA detection at attomolar level. Anal. Chem. 86 (16), 8098–8105.

Zhang, X., Liu, C., Sun, L., Duan, X., Li, Z., 2015. Lab on a single microbead: an ultrasensitive detection strategy enabling microRNA analysis at the single-molecule level. Chem. Sci. 6 (11), 6213–6218.

Zhang, Y., Zhang, L., Sun, J., Liu, Y., Ma, X., Cui, S., Ma, L., Xi, J.J., Jiang, X., 2014c. Point-of-care multiplexed assays of nucleic acids using microcapillary-based loop-mediated isothermal amplification. Anal. Chem. 86 (14), 7057–7062.

Zhao, G., Guan, Y., 2010. Polymerization behavior of Klenow fragment and Taq DNA polymerase in short primer extension reactions. Acta Biochim. Et Biophys. Sin. 42 (10), 722–728.

Zhao, Y., Chen, F., Li, Q., Wang, L., Fan, C., 2015. Isothermal amplification of nucleic acids. Chem. Rev. 115 (22), 12491–12545.

Zhao, Y., Chen, F., Zhang, Q., Zhao, Y., Zuo, X., Fan, C., 2014. Polymerase/nicking enzyme synergetic isothermal quadratic DNA machine and its application for one-step amplified biosensing of lead (II) ions at femtomole level and DNA methyltransferase. NPG Asia Mater. 6 (9), e131.

Zhou, X., Su, Q., Xing, D., 2012. An electrochemiluminescent assay for high sensitive detection of mercury (II) based on isothermal rolling circular amplification. Anal. Chim. Acta 713, 45–49.

Zhu, X., Zhou, X., Xing, D., 2011. Ultrasensitive and selective detection of mercury (II) in aqueous solution by polymerase assisted fluorescence amplification. Biosens. Bioelectron. 26 (5), 2666–2669 (Yu).